Atmos. Chem. Phys., 24, 11701–11716, 2024
https://doi.org/10.5194/acp-24-11701-2024


Atmospheric Chemistry and Physics
Open Access
EGU



# Nocturnal atmospheric synergistic oxidation reduces the formation of low-volatility organic compounds from biogenic emissions

**Han Zang[1], Zekun Luo[1], Chenxi Li[1], Ziyue Li[1], Dandan Huang[2], and Yue Zhao[1]**

[1]School of Environmental Science and Engineering, Shanghai Jiao Tong University, Shanghai, 200240, China
[2]Shanghai Academy of Environmental Sciences, Shanghai, 200233, China

**Correspondence:** Dandan Huang (huangdd@saes.sh.cn) and Yue Zhao (yuezhao20@sjtu.edu.cn)

Received: 14 April 2024 – Discussion started: 17 April 2024
Revised: 8 August 2024 – Accepted: 22 August 2024 – Published: 21 October 2024

**Abstract.** Volatile organic compounds (VOCs) are often subject to synergistic oxidation by different oxidants in the atmosphere. However, the exact synergistic-oxidation mechanism of atmospheric VOCs and its role in particle formation remain poorly understood. In particular, the reaction kinetics of the key reactive intermediates, organic peroxy radicals ($RO_2$), during synergistic oxidation is rarely studied. Here, we conducted a combined experimental and kinetic modeling study of the nocturnal synergistic oxidation of $\alpha$-pinene (the most abundant monoterpene) by $O_3$ and $NO_3$ radicals as well as its influences on the formation of highly oxygenated organic molecules (HOMs) and particles. We find that in the synergistic $O_3 + NO_3$ regime, where OH radicals are abundantly formed via decomposition of ozonolysis-derived Criegee intermediates, the production of $C_xH_yO_z$ HOMs is substantially suppressed compared to that in the $O_3$-only regime, mainly because of the depletion of $\alpha$-pinene $RO_2$ derived from ozonolysis and OH oxidation by those arising from $NO_3$ oxidation via cross reactions. Measurement–model comparisons further reveal that the cross-reaction rate constants of $NO_3$-derived $RO_2$ with $O_3$-derived $RO_2$ are on average 10–100 times larger than those of $NO_3$-derived $RO_2$ with OH-derived $RO_2$. Despite a strong production of organic nitrates in the synergistic-oxidation regime, the substantial decrease in $C_xH_yO_z$ HOM formation leads to a significant reduction in ultralow- and extremely low-volatility organic compounds, which significantly inhibits the formation of new particles. This work provides valuable mechanistic and quantitative insights into the nocturnal synergistic-oxidation chemistry of biogenic emissions and will help to better understand the formation of low-volatility organic compounds and particles in the atmosphere.

## 1 Introduction

Earth's atmosphere is a complex oxidizing environment in which multiple oxidants coexist. During nighttime, $NO_3$ radicals (generated by the reaction of $NO_2$ and $O_3$) and $O_3$ contribute significantly to the oxidation of volatile organic compounds (VOCs) (Huang et al., 2019), while during daytime, the fast photolysis of $NO_3$ radicals and rapid photochemical formation of OH radicals and $O_3$ make the latter two the major oxidants for VOCs (Zhang et al., 2018). Therefore, the degradation of ambient VOCs is subject to concurrent oxidation by different oxidants. Gas-phase oxidation of VOCs from biogenic emissions (BVOCs) by these major atmospheric oxidants produces a key type of reactive intermediate, organic peroxy radicals ($RO_2$), a portion of which can undergo fast autoxidation, forming a class of highly oxygenated organic molecules (HOMs) with low volatilities (Jokinen et al., 2014; Mentel et al., 2015; Berndt et al., 2016; Zhao et al., 2018; Iyer et al., 2021; Shen et al., 2022; Ehn et al., 2014). HOMs typically contain six or more oxygen atoms and play a key role in the formation of atmospheric new particles and secondary organic aerosol (SOA) (Kirkby et al., 2016; Berndt et al., 2018; Zhao et al., 2018; Ehn et al., 2014; Bianchi et al., 2019), which have important influences on air quality (Huang et al., 2014), public health (Pye et al., 2021), and Earth's radiative forcing (Shrivastava et al., 2017).

Due to the complexity of oxidation mechanisms of BVOCs, previous laboratory studies typically featured only one oxidant and a single SOA precursor (Berndt et al., 2016; Berndt, 2021; Claflin et al., 2018; Iyer et al., 2021; Boyd et al., 2015). However, the synergistic oxidation by different oxidants may significantly alter the fate of $RO_2$ intermediates, therefore influencing the formation of HOMs and SOA (Bates et al., 2022). Recently, a field study at a boreal forest site in Finland observed a series of nitrate-containing HOM dimers from the coupled $O_3 + NO_3$ oxidation of monoterpenes (Zhang et al., 2020). At the same site, Lee et al. (2020) found that the synergistic oxidation of BVOCs by OH radicals and $O_3$ contributed to the largest fraction of SOA. These studies suggest that the synergistic oxidation of BVOCs by different oxidants plays an important role in the formation of HOMs and SOA in the atmosphere and highlight the need to investigate the synergistic-oxidation mechanisms of BVOCs for a better representation of atmospheric particle formation.

Several laboratory studies have attempted to address the role of synergistic oxidation of BVOCs in the formation of new particles and SOA (Kenseth et al., 2018; Inomata, 2021; Liu et al., 2022; Li et al., 2024). Kenseth et al. (2018) identified a suite of dimer esters in flow tube experiments that can be only formed from the $OH + O_3$ synergistic oxidation of $\beta$-pinene. These dimers exhibit extremely low volatility and contributed 5.9 %–25.4 % to the total $\beta$-pinene SOA. Similarly, Inomata (2021) found that the presence of OH radicals during $\alpha$-pinene ozonolysis is a key factor in the production of low-volatility organic species and significantly promotes new particle formation (NPF). On the other hand, the addition of $O_3$ in the monoterpene photooxidation system also significantly increases the SOA mass yield (Liu et al., 2022). In addition, a recent chamber study by Bates et al. (2022) showed that the synergistic oxidation of $\alpha$-pinene by $NO_3$ radicals and $O_3$ can significantly enhance the SOA yield compared to the $NO_3 + \alpha$-pinene regime, which has nearly 0 % SOA yield (Fry et al., 2014; Hallquist et al., 1999; Mutzel et al., 2021), and they revealed that the SOA yield in the $NO_3 + O_3$ oxidation system largely depends on the $RO_2$ fates. Most recently, Li et al. (2024) found that during $\alpha$-pinene ozonolysis, the presence of nitrooxy $RO_2$ radicals formed from $NO_3$ oxidation can significantly suppress the production of ultralow-volatility organic compounds (ULVOCs) and thereby NPF. These laboratory studies together provide growing evidence that synergistic oxidation of BVOCs by different oxidants has profound impacts on atmospheric particle formation. However, the specific synergistic mechanisms of different oxidants and oxidation pathways remain obscure. Although a few studies underscored the importance of the $RO_2$ fates (Bates et al., 2022; Li et al., 2024), the exact interactions between $RO_2$ species derived from different oxidants are still unclear, and quantitative constraints on the reaction rate of different $RO_2$ species are quite limited.

Here we conducted an investigation of the synergistic $O_3 + NO_3$ oxidation of $\alpha$-pinene, one of the most abundant monoterpenes in the atmosphere, using a combination of laboratory experiments and detailed kinetic modeling and focusing on the fate of $RO_2$ intermediates arising from different oxidation pathways. The $\alpha$-pinene oxidation experiments were conducted in a custom-built flow reactor. The molecular composition of $RO_2$ species and HOMs in different oxidation regimes was characterized using a chemical-ionization atmospheric-pressure interface time-of-flight mass spectrometer (CI-APi-ToF MS) employing a nitrate ion source. The measured distributions of specific $RO_2$ and HOMs across different oxidation regimes were fitted with a kinetic model using Master Chemical Mechanisms (MCM v3.3.1) updated with recent advances of $\alpha$-pinene $RO_2$ chemistry (Wang et al., 2021; Iyer et al., 2021; Shen et al., 2022; Zang et al., 2023), which allows for quantitative constraints on $RO_2$ kinetics and synergistic-oxidation mechanisms. Atmospheric relevance of the experimental results was evaluated by modeling the investigated oxidation chemistry under typical nocturnal atmospheric conditions.

## 2 Materials and methods

### 2.1 Flow tube experiments

Experiments of $\alpha$-pinene oxidation in different regimes (i.e., synergistic $O_3 + NO_3$ oxidation vs. the $O_3$-only regime) were carried out under room temperature (298 K) and dry (relative humidity $< 5$ %) conditions in a custom-built flow tube reactor (FTR; Fig. S1 in the Supplement). $O_3$ and $NO_2$ were added to a glass tube (Fig. S1) to form the $NO_3$ radical and its precursor, $N_2O_5$:

$$NO_2 + O_3 \rightarrow NO_3 + O_2, \quad \text{(R1)}$$

$$NO_3 + NO_2 \leftrightarrow N_2O_5. \quad \text{(R2)}$$

$O_3$ was generated by passing a flow of ultrahigh-purity (UHP) $O_2$ (Shanghai Maytor Special Gas Co., Ltd.) through a quartz tube housing a pen-ray mercury lamp (UV-S2, UVP Inc.), and its concentration was measured by an ozone analyzer (T400, API). $NO_2$ was obtained from a gas cylinder (15.6 ppm, Shanghai Weichuang Standard Gas Co., Ltd.). The initial $NO_2$ concentration in the flow tube was 4.5–6.4 ppb. To prevent the titration of $NO_3$ radicals by NO, all the experiments were performed without the addition of NO. The total airflow in the $NO_3$ generation glass tube was 0.6 and 0.4 L min$^{-1}$ for the gas-phase HOM and SOA formation experiments, respectively. The produced $N_2O_5$ and $NO_3$ radicals, as well as the excessive $O_3$, were added into the FTR to initiate $\alpha$-pinene oxidation. For the $O_3$-only experiments, only $O_3$ was added into FTR.

The $\alpha$-pinene gas was generated by evaporating a defined volume of its liquid (99 %, Sigma-Aldrich) into a cleaned and evacuated canister (SilcoCan, Restek) and then added

into the FTR through a movable injector at a flow rate of 22–108 mL min$^{-1}$. The initial concentration of $\alpha$-pinene in the flow reactor ranged from 100–500 ppb. In some experiments, the gas of cyclohexane ($\sim$ 100 ppm), which was generated by bubbling a gentle flow of UHP $N_2$ through its liquid (liquid chromatography–mass spectrometry grade, CNW), was added into the flow reactor as a scavenger of OH radicals formed from $\alpha$-pinene ozonolysis.

For experiments characterizing the formation of HOMs, the total airflow in the FTR was 10.8 L min$^{-1}$ and the residence time was 25 s. The short reaction time and the small amount of reacted $\alpha$-pinene (see Table S1 in the Supplement) in these experiments prevented the formation of particles. For the experiments characterizing the formation of SOA particles, a larger FTR was used, with a total airflow of 5 L min$^{-1}$ and a residence time of 180 s. A summary of the conditions including the simulated concentrations of $NO_2$, $N_2O_5$, and $NO_3$ radicals, as well as the concentration of $\alpha$-pinene oxidized by each oxidant in different experiments, is given in Table S1.

The gas-phase $RO_2$ radicals and closed-shell products were measured using a nitrate-based CI-APi-ToF MS (abbreviated as nitrate CIMS, chemical-ionization mass spectrometer; Aerodyne Research, Inc.), which has been described in detail previously (Zang et al., 2023). A long-ToF MS with a mass resolution of $\sim$ 10 000 was used here. The mass spectra within the $m/z$ range of 50–700 were analyzed using the tofTools package developed by Junninen et al. (2010) based on MATLAB. The total ion counts (TICs) with values of (5.9–6.2) $\times 10^4$ cps (counts per second) are similar under different reaction conditions. In this study, we assume that the $C_xH_yO_z$ HOMs derived from ozonolysis and OH oxidation of $\alpha$-pinene exhibit the same sensitivity in nitrate CIMS. However, the highly oxygenated organic nitrates (ONs) may have a significantly lower sensitivity compared to the $C_xH_yO_z$ HOM counterparts, given that the substitution of the –OOH or –OH groups by the –$ONO_2$ group in the molecule would reduce the number of H-bond donors, which is a key factor in determining the sensitivity of nitrate CIMS (Shen et al., 2022; Hyttinen et al., 2015). Recently, Li et al. (2024) used CI-Orbitrap with ammonium or nitrate reagent ions to detect oxygenated organic molecules in the synergistic $O_3 + NO_3$ regime and found that both the ion intensity of ONs and their signal contribution to the total dimers were much lower when using nitrate as reagent ions.

A scanning mobility particle sizer (SMPS, TSI), consisting of an electrostatic classifier (model 3082); a condensation particle counter (model 3756); and a long or nano differential mobility analyzer (model 3081 and 3085) with a measurable size range of 4.6–156.8 nm or 14.6–661.2 nm, respectively, was employed to monitor the formation of particles in the flow tube. During the HOM formation experiments, even under conditions with the highest initial $\alpha$-pinene concentration (500 ppb), only a tiny number of particles was formed, with mass concentrations of (6.4 $\pm$ 1.7) $\times 10^{-3}$ and (1.0 $\pm$ 0.4) $\times 10^{-2}$ µg m$^{-3}$ and number concentrations of 574 $\pm$ 148 and 256 $\pm$ 68 cm$^{-3}$ in the $O_3$-only (experiment 5) and $O_3 + NO_3$ (experiment 11) regimes, respectively. These results suggest that the formation of SOA particles in the HOM formation experiments is negligible and would have no significant influence on the fate of $RO_2$ and closed-shell products.

## 2.2 Estimation of HOM volatility

A modified composition-activity method was used to estimate the saturation mass concentration ($C^*$) of HOMs in this study according to the approach developed by Li et al. (2016):

$$\log_{10}C^* = \left(n_C^0 - n_C\right)b_C - n_O b_O - 2\frac{n_C n_O}{n_C + n_O}b_{co} - n_N b_N - n_S b_S, \quad (1)$$

where $n_C^0$ is the reference carbon number; $n_C$, $n_O$, $n_N$, and $n_S$ are the atomic numbers of carbon, oxygen, nitrogen, and sulfur, respectively; $b_C$, $b_O$, $b_N$, and $b_S$ are the contribution of each atom to $\log_{10}C^*$, respectively; and $b_{co}$ is the carbon–oxygen nonideality (Donahue et al., 2011). These $b$ values were provided by Li et al. (2016).

It should be noted that the CHON compounds used in the data set by Li et al. (2016) are mostly amines, amides, and amino acids and only contain a limited number of ONs (0.07 %). Since different types of CHON compounds have very different vapor pressures (Isaacman-VanWertz and Aumont, 2021), this formula-based approach can be biased to estimate the $C^*$ of ONs. Considering that the –$ONO_2$ and –OH groups have similar impacts on vapor pressure and that the CHON species are predominantly ONs in our study, all –$ONO_2$ groups are treated as –OH groups during the estimation of vapor pressure (Daumit et al., 2013; Isaacman-VanWertz and Aumont, 2021).

Gas-phase HOMs are grouped into five classes based on their $\log_{10}C^*$ (Donahue et al., 2012; Bianchi et al., 2019; Schervish and Donahue, 2020), that is, ULVOCs ($\log_{10}C^* < -8.5$), extremely low-volatility organic compounds (ELVOCs; $-8.5 < \log_{10}C^* < -4.5$), low-volatility organic compounds (LVOCs; $-4.5 < \log_{10}C^* < -0.5$), semi-volatile organic compounds (SVOCs; $-0.5 < \log_{10}C^* < 2.5$), and intermediate-volatility organic compounds (IVOCs; $2.5 < \log_{10}C^* < 6.5$).

## 2.3 Kinetic model simulations

Model simulations of specific $RO_2$ radicals and closed-shell HOMs formed in different oxidation regimes were performed to constrain the reaction kinetics and mechanisms using the Framework for 0-D Atmospheric Modeling (F0AM v4.1) (Wolfe et al., 2016), which employs MCM v3.3.1 (Jenkin et al., 2015). The $\alpha$-pinene oxidation mechanism was updated with state-of-the-art knowledge regarding the chem-

istry of $RO_2$ autoxidation and cross reactions forming HOM monomers and dimers, respectively (Zhao et al., 2018; Wang et al., 2021; Iyer et al., 2021; Shen et al., 2022). The detailed updates have been described in our previous study (Zang et al., 2023). In particular, the formation and subsequent reactions of the ring-opened primary $C_{10}H_{15}O_4$ $RO_2$, the highly oxygenated acyl $RO_2$, and the $C_{10}H_{15}O_2$ $RO_2$ arising from H abstraction by OH radicals during $\alpha$-pinene ozonolysis are included in the model according to recent studies (Iyer et al., 2021; Zhao et al., 2022; Zang et al., 2023; Shen et al., 2022).

To investigate the synergistic reactions of $RO_2$ derived from the oxidation of $\alpha$-pinene by different oxidants, we added the cross reactions of the primary nitrooxy $RO_2$ derived from $NO_3$ oxidation ($^{NO_3}RO_2$), i.e., $C_{10}H_{16}NO_5$ $RO_2$, with $RO_2$ derived from ozonolysis ($^{CI}RO_2$) and OH oxidation ($^{OH}RO_2$). Recently, Zhao et al. (2018) revealed the bulk rate constant for $^{CI}RO_2$ and $^{OH}RO_2$ self-reactions/cross reactions to be $2 \times 10^{-12}$ cm$^3$ molec.$^{-1}$ s$^{-1}$, and Bates et al. (2022) constrained the rate constant for $^{NO_3}RO_2$ self-reactions/cross reactions to be $1 \times 10^{-13}$–$1 \times 10^{-12}$ cm$^3$ molec.$^{-1}$ s$^{-1}$. In the present study, the default rate constant for $^{NO_3}RO_2 + {}^{CI}RO_2$ was set to $2 \times 10^{-12}$ cm$^3$ molec.$^{-1}$ s$^{-1}$, the same as for self-reactions/cross reactions of $^{CI}RO_2$ and $^{OH}RO_2$. The default rate constant for $^{NO_3}RO_2 + {}^{NO_3}RO_2$ was set to $1 \times 10^{-12}$ cm$^3$ molec.$^{-1}$ s$^{-1}$. The ratio of the cross-reaction rate constant of $^{NO_3}RO_2 + {}^{CI}RO_2$ to that of $^{NO_3}RO_2 + {}^{OH}RO_2$ was tuned to achieve a good measurement–model agreement for the distribution of specific $RO_2$ and HOMs across different oxidation regimes. Recent studies suggested that the ROOR′ dimer formation rates from the highly oxygenated $RO_2$ are fast (Berndt et al., 2018; Molteni et al., 2019). As a result, a relatively high dimer formation branching ratio of 50 % was used for different $RO_2$ types (e.g., $^{CI}RO_2$, $^{OH}RO_2$, $^{NO_3}RO_2$) in the model, except for the reaction of $^{NO_3}RO_2 + {}^{NO_3}RO_2$, for which ROOR′ dimer formation was not considered, given the extremely low signals of $CHON_2$ dimers observed in the synergistic-oxidation regime (see Sect. 3.1). With these default kinetic parameters, the $RO_2$ bimolecular lifetimes were predicted to be 10.9–25.9 s in the $O_3$-only regime and 8.4–11.8 s in the $O_3 + NO_3$ regime in the HOM formation experiments. Considering that the $RO_2$ cross-reaction kinetics remain highly uncertain, sensitivity analyses were performed to evaluate their influences on the results in this study (see Sect. 3.2). Previous studies indicated that the primary $^{NO_3}RO_2$ radicals arising from $\alpha$-pinene are prone to lose the nitrate group and form pinonaldehyde with high volatility (Kurtén et al., 2017; Fry et al., 2014). Therefore, we did not consider the autoxidation of primary $^{NO_3}RO_2$ in the model. Considering the presence of $NO_2$ in the experiments, the reactions of $RO_2 + NO_2 \leftrightharpoons ROONO_2$ were also included in the model (Zang et al., 2023).

## 3 Results and discussion

### 3.1 Molecular distribution of $RO_2$ and HOMs in the synergistic-oxidation regime

The abundance of gas-phase $RO_2$ species and HOMs in different oxidation regimes is shown in Fig. 1a. The species signals are normalized by the total reacted $\alpha$-pinene in each regime. Compared to the $O_3$-only regime, the normalized signals of total $RO_2$ and HOMs decrease by 63 %–68 % in the synergistic $O_3 + NO_3$ regime. Although $NO_3$ oxidation accounts for a considerable fraction of reacted $\alpha$-pinene in the synergetic oxidation regime, the signal contributions of HOM ONs are not significant. This might be due to the low sensitivity of nitrate CIMS to the ONs formed involving $NO_3$ oxidation (Sect. 2.1). Although there remain considerable uncertainties in instrument sensitivities for different compounds, sensitivity analyses suggest that varying the CIMS sensitivities to $RO_2$ and HOMs by a factor of 10 would not significantly influence their relative distribution across different oxidation regimes (see Sect. S1 in the Supplement for details).

Note that the initial concentrations of $\alpha$-pinene and $O_3$ in the two oxidation regimes were the same. In addition, model simulations show that in the synergistic $O_3 + NO_3$ regime, over 97 % of OH radicals react with $\alpha$-pinene and the depletion of OH by $NO_2$ is minor (0.2 %–1.3 %). Also, $NO_3$ radicals almost entirely (over 98.5 %) react with $\alpha$-pinene, and their reaction with $RO_2$ has negligible influence on the fate of $RO_2$ (Fig. S2). Meanwhile, the depletion of acyl $RO_2$ by $NO_2$ only leads to a small reduction (4 %–5 % and 7 %–12 %, respectively) in total $C_xH_yO_z$ HOM monomers and dimers in the synergistic regime compared to the $O_3$-only regime. As a result, the strong reduction in $C_xH_yO_z$ HOM formation due to the presence of $NO_3$ oxidation is likely mainly due to (i) the fast competitive consumption of $\alpha$-pinene by $NO_3$ radicals, which leads to a reduction in the reacted $\alpha$-pinene by $O_3$ ($\Delta[\alpha\text{-pinene}]_{O_3}$, Fig. S3) and thereby $C_xH_yO_z$ HOM signals, and (ii) the cross reactions of $^{CI}RO_2$ or $^{OH}RO_2$ with $^{NO_3}RO_2$, which suppress the autoxidation and self-reactions/cross reactions of $^{CI}RO_2$ and $^{OH}RO_2$ to form $C_xH_yO_z$ HOMs.

To quantify the contribution of cross reactions of $^{NO_3}RO_2$ with $^{CI}RO_2/{}^{OH}RO_2$ to the suppressed formation of $C_xH_yO_z$ HOMs in the synergistic-oxidation regime, $C_xH_yO_z$ HOM signals shown in Fig. 1a are first normalized to $\Delta[\alpha\text{-pinene}]_{O_3}$ in each oxidation regime and then compared between different oxidation regimes (see Fig. 1b). Notably, after excluding the influence of reduced $\Delta[\alpha\text{-pinene}]_{O_3}$, the $C_xH_yO_z$ HOM signals still drop by 32 %–33 % in the $O_3 + NO_3$ regime compared to those in the $O_3$-only regime, indicating a significant contribution of the coupled reactions between $^{NO_3}RO_2$ and $^{CI}RO_2$ or $^{OH}RO_2$ to suppressed $C_xH_yO_z$ HOM formation.

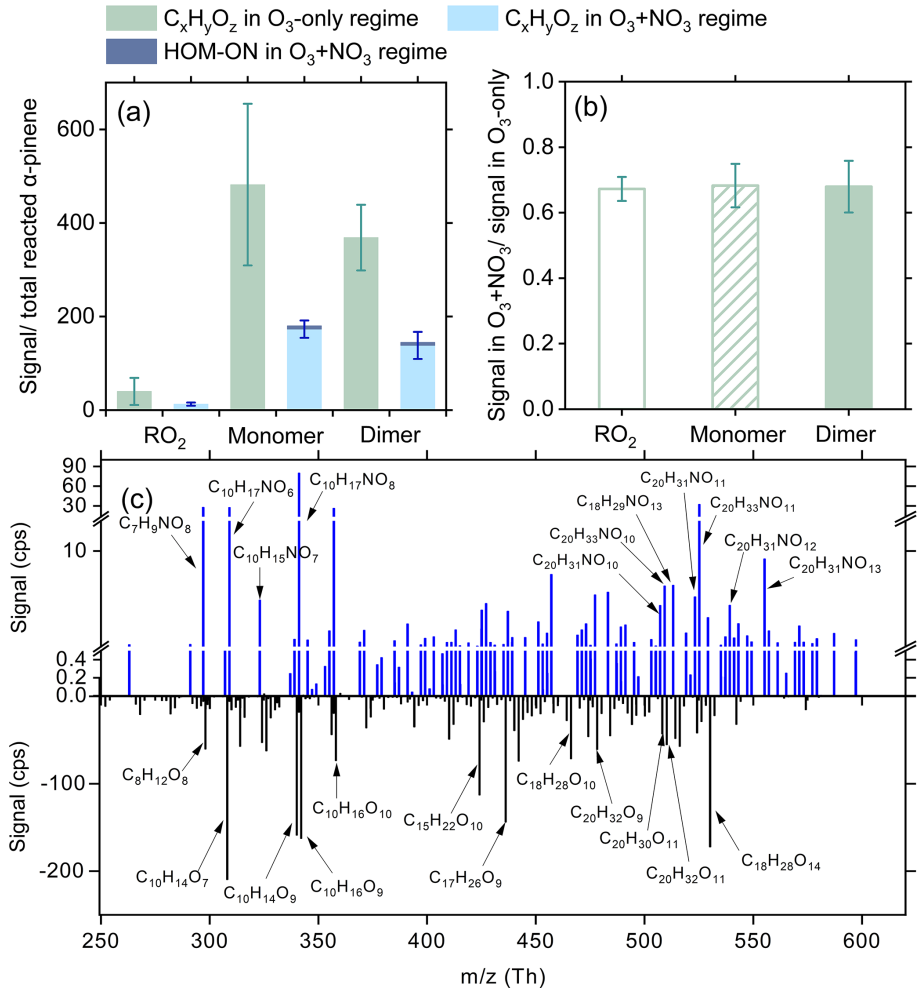


**Figure 1.** Distributions of $RO_2$ and HOMs in the $O_3$-only and $O_3 + NO_3$ regimes. **(a)** Signals of total $RO_2$, as well as HOM monomers and dimers normalized by the total reacted $\alpha$-pinene in each oxidation regime (experiments 1–5, 7–11). **(b)** Relative changes in the normalized signals of $C_xH_yO_z$ HOMs in the $O_3 + NO_3$ regime vs. the $O_3$-only regime. Ion signals are normalized to $\Delta[\alpha\text{-pinene}]_{O_3}$ in each oxidation regime to highlight the suppression effect of the synergistic chemistry between $^{NO_3}RO_2$ and $^{CI}RO_2$ or $^{OH}RO_2$ on $C_xH_yO_z$ HOM formation. **(c)** Difference mass spectrum between the two oxidation regimes. The positive and negative peaks indicate the species with enhanced and decreased formation in the $O_3 + NO_3$ regime compared to the $O_3$-only regime, respectively.

Figure 1c shows a difference mass spectrum, highlighting the changes in species distribution between the two oxidation regimes. Almost all $C_xH_yO_z$ HOM species decrease significantly in the $O_3 + NO_3$ regime compared to the $O_3$-only regime. Furthermore, a large set of HOM ON species are formed, despite their relatively low signals. It should be noted that no obvious signals of highly oxygenated $^{NO_3}RO_2$ ($C_{10}H_{16}NO_x$, $x \geq 6$) were observed by nitrate CIMS in the $O_3 + NO_3$ oxidation system. One possible reason is that nitrate CIMS exhibits relatively low sensitivity to the ONs. Secondly, the instrument's mass resolution is not high enough to differentiate the mass closure between some of $^{NO_3}RO_2$ and $C_xH_yO_z$ HOMs with strong peaks (Table S2), limiting the detection of $^{NO_3}RO_2$ species. Furthermore, previous studies revealed that the primary $^{NO_3}RO_2$ radicals (i.e., $C_{10}H_{16}NO_5$ $RO_2$) in the $\alpha$-pinene + $NO_3$ system mainly react to form pinonaldehyde (Kurtén et al., 2017; Perraud et al., 2010). It is likely that only a very small amount of $^{NO_3}RO_2$ can undergo intramolecular H shift and $O_2$ addition to form highly oxygenated $^{NO_3}RO_2$. It should be pointed out that although the primary $C_{10}H_{16}NO_5$ $RO_2$ species arising from $NO_3$ oxidation may not undergo fast autoxidation, they tend to efficiently terminate $^{CI}RO_2$ and/or $^{OH}RO_2$ and suppress the formation of $C_xH_yO_z$ HOMs.

As shown in Fig. 1c, although several closed-shell monomeric HOM ONs have been observed in the synergistic-oxidation regime, only a few of them exhibit relatively high signals. Among them, $C_{10}H_{17}NO_8$ may be formed by the autoxidation of $C_{10}H_{16}NO_6$ $RO_2$ derived from the intramolecular H shift in primary $^{NO_3}RO$ radicals

($C_{10}H_{16}NO_4$). In addition, although CI is a soft ionization method, the fragmentation of chemically labile species still occurs during the ionization in nitrate CIMS. It is possible that some of the dimeric HOM ONs are fragmented to $C_{10}H_{17}NO_8$ during measurements with nitrate CIMS. In a recent study by Li et al. (2024), $C_{10}H_{17}NO_8$ was also identified during the synergistic oxidation of $\alpha$-pinene by $O_3$ and $NO_3$. However, the exact origin of this species remains to be determined.

The $C_{20}$ dimers with only one nitrogen atom are very likely to be formed from the cross reactions of $^{CI}RO_2$ or $^{OH}RO_2$ with $^{NO_3}RO_2$, which provides direct evidence for the synergistic $RO_2$ chemistry in the $O_3 + NO_3$ regime. The $CHON_2$ dimers were also observed in the $O_3 + NO_3$ regime, despite their signals that were much lower than those of CHON dimers, which is different from the recent studies by Bates et al. (2022) and Li et al. (2024), which found $CHON_2$ dimers account for an important fraction of the total dimer signals in the synergistic-oxidation regime. A potential explanation for this discrepancy is the difference in the instrument sensitivity in these studies (Sect. 2.1). In general, the nitrate CIMS has lower sensitivities to ONs than to the $C_xH_yO_z$ HOM counterparts (Shen et al., 2022; Hyttinen et al., 2015). Bates et al. (2022) used $CF_3O^-$ as the reagent ion of CIMS. Its sensitivity to ONs might be significantly higher than the nitrate ion. In addition, Li et al. (2024) observed a significantly lower signal contribution of $CHON_2$ dimers using CI-Orbitrap with nitrate reagent ions than with ammonium ions. Despite both using nitrate reagent ions, the nitrate CI-Orbitrap in Li et al. (2024) possibly exhibits higher sensitivities to ONs than the nitrate CIMS in our study.

### 3.2 Synergistic reaction efficiencies of different $RO_2$ species

In the $O_3 + NO_3$ regime, synergistic reactions are likely to occur between $^{CI}RO_2$, $^{OH}RO_2$, and $^{NO_3}RO_2$. Figure 2 shows the $\Delta[\alpha\text{-pinene}]_{O_3}$-normalized signal ratios of specific $C_{10}$ $RO_2$ as well as their related $C_xH_yO_z$ HOM monomers and dimers in the synergistic $O_3 + NO_3$ regime vs. the $O_3$-only regime. It should be noted that the second-generation oxidation processes are strongly inhibited by the excess of $\alpha$-pinene in this study; thus the predominant type of $RO_2$ observed here is primary $RO_2$. Model simulations show that the H abstraction of $\alpha$-pinene by OH radicals contributes less than 2 % to the formation of $C_{10}H_{15}O_x$ $RO_2$ and related HOMs under different experimental conditions (Fig. S5). Therefore, $C_{10}H_{15}O_x$ $RO_2$ observed in this study are primarily $^{CI}RO_2$. Notably, the $^{CI}RO_2$ ($C_{10}H_{15}O_x$) and related $C_{10}H_{14}O_x$ HOMs decrease by $\sim$ 20 %–80 % in the $O_3 + NO_3$ regime (Fig. 2a and b), while the decreasing extent of $^{OH}RO_2$ ($C_{10}H_{17}O_x$) and related $C_{10}H_{18}O_x$ HOMs are significantly smaller (0 %–30 %). In particular, some of the most oxygenated $C_{10}H_{17}O_x$ $RO_2$ and $C_{10}H_{18}O_x$ HOMs ($x \geq 9$) even increase unexpectedly in the synergistic-oxidation regime. For the $C_{10}H_{16}O_x$ HOMs that can be derived from the self-reactions/cross reactions of both $^{CI}RO_2$ and $^{OH}RO_2$, their reductions are at a medium level. Because of the very small contribution of acyl $RO_2$ to the total $C_{10}$ $RO_2$ (0.4 %) (Zang et al., 2023), their consumption by $NO_2$ leads to a reduction of less than 2 % in the $C_{10}$ $^{CI}RO_2$ signals. Therefore, the more significant decrease in signals of $^{CI}RO_2$ and related HOMs as compared to the OH-derived ones in the synergistic $O_3 + NO_3$ regime is primarily due to the more efficient cross reactions of $^{NO_3}RO_2$ with $^{CI}RO_2$ than with $^{OH}RO_2$. Because a large amount of $^{CI}RO_2$ is terminated by $^{NO_3}RO_2$, less $^{CI}RO_2$ is available to terminate $^{OH}RO_2$. As a result, more $^{OH}RO_2$ can undergo autoxidation to form highly oxygenated $C_{10}H_{17}O_x$ $RO_2$ and $C_{10}H_{18}O_x$ HOMs ($x \geq 9$), leading to an increase in signals of these species. Consistently, the signals of $C_{20}$ HOM dimers decrease by $\sim$ 20 %–40 % in the $O_3 + NO_3$ regime compared to those in the $O_3$-only regime, and the signal reduction in dimers ($C_{20}H_{30}O_x$) formed by $^{CI}RO_2$ is slightly larger than that of the dimers ($C_{20}H_{34}O_x$) arising from $^{OH}RO_2$ (Fig. 2c). Note that the highly oxygenated $C_{20}H_{34}O_x$ dimers ($x \geq 13$) that can be formed from self-reactions/cross reactions of $C_{10}H_{17}O_x$ $RO_2$ ($x \geq 9$) are not observed in this study, likely due to their low abundance and the limitation of instrument sensitivity.

The above results are somewhat different from the most recent study by Li et al. (2024), which found that the measured $C_{10}H_{15}O_x$ $RO_2$ increased slightly with $NO_3$ radicals, while $C_{10}H_{17}O_{5,7}$ $RO_2$ from OH chemistry decreased by a factor of 9. Li et al. (2024) indicated that additional $C_{10}H_{15}O_x$ could be produced from the H-abstraction pathway of $NO_3$ oxidation of $\alpha$-pinene. However, in the monoterpene oxidation system, the rate constant for H abstraction by $NO_3$ radicals is $(4\text{–}10) \times 10^{-17}$ cm$^3$ molec.$^{-1}$ s$^{-1}$, which is $10^3$–$10^4$ times lower than that for the $NO_3$ addition channel (Martinez et al., 1998). Besides this, the subsequent reactions of $RO_2$ species formed from H abstraction by $NO_3$ radicals should be very similar to those derived from H abstraction by OH radicals, which was found to be not important for $C_xH_yO_z$ HOM formation in the absence of NO (Zang et al., 2023). Therefore, the H abstraction of $\alpha$-pinene by $NO_3$ radicals would have a negligible influence on $C_{10}H_{15}O_x$ formation. As Li et al. (2024) used a low $\alpha$-pinene concentration and relatively high $O_3$ and $NO_3$ concentrations in their experiments, the secondary oxidation of aldehydes, such as the substantially formed pinonaldehyde, by $NO_3$ radicals might be important, which could contribute to the additional formation of $C_{10}H_{15}O_x$ $RO_2$. However, as noted above, the second-generation oxidation processes are strongly inhibited due to the excess of $\alpha$-pinene in this study; therefore the formation of secondary $C_{10}H_{15}O_x$ $RO_2$ is not important.

In addition, Li et al. (2024) reported that the fraction of $\alpha$-pinene oxidized by OH radicals decreased from 44 % in the $O_3$ oxidation system to 6 % in the $O_3 + NO_3$ system, mainly due to the depletion of OH radicals by $NO_2$ and the competitive consumption of $\alpha$-pinene by $NO_3$ radicals, which re-

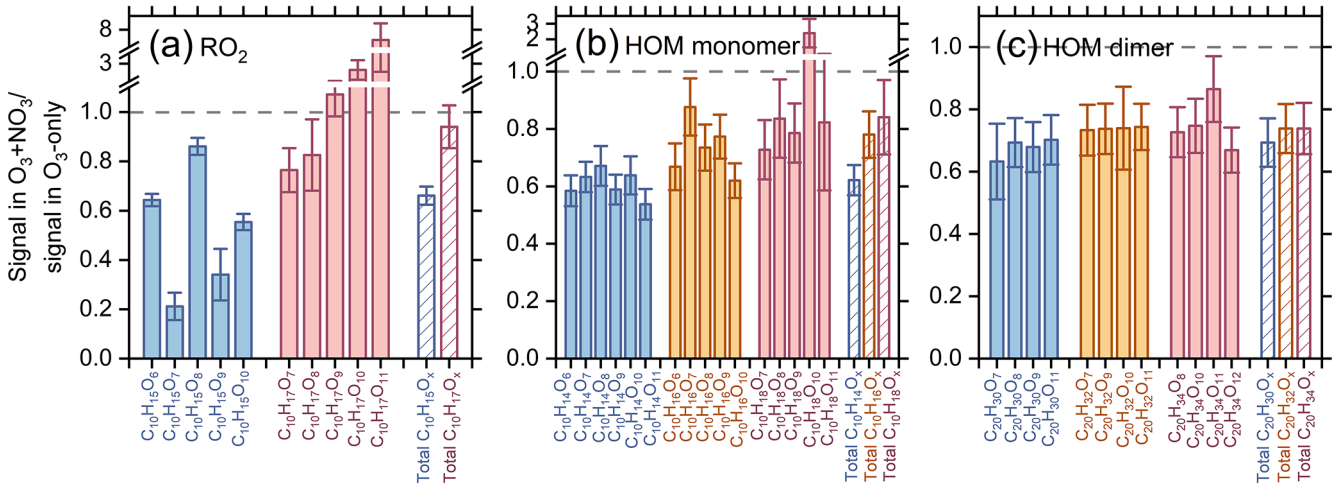


**Figure 2.** Normalized signal ratios of **(a)** specific and total $C_{10}H_{15,17}O_x$ $RO_2$ radicals, as well as **(b–c)** their related **(b)** $C_{10}$ HOM monomers and **(c)** $C_{20}$ HOM dimers in the $O_3 + NO_3$ regime vs. the $O_3$-only regime (experiments 1–5 and 7–11). Ion signals observed in each oxidation regime are normalized to $\Delta[\alpha\text{-pinene}]_{O_3}$.

sulted in a significant decrease in $C_{10}H_{17}O_{5,7}$ radicals from OH chemistry as observed in their experiments. However, in the present study, because of the excess of $\alpha$-pinene, over 97 % of OH radicals react with $\alpha$-pinene and the depletion of OH by $NO_2$ is minor (0.2 %–1.3 %) in the $O_3 + NO_3$ regime. The reduction in the reacted $\alpha$-pinene by OH radicals is less than 10 % compared to the $O_3$-only regime. As a result, a smaller decrease in $C_{10}H_{17}O_{5,7}$ radicals was observed in our study.

To gain quantitative constraints on the relative reaction efficiency of $^{NO_3}RO_2 + {}^{CI}RO_2$ vs. $^{NO_3}RO_2 + {}^{OH}RO_2$ (i.e., $k_{NO_3+CI}/k_{NO_3+OH}$), the signal ratios of $C_{10}$ $^{CI}RO_2$ and $^{OH}RO_2$ as well as their related $C_{10}$ HOMs in the synergistic-oxidation regime vs. the $O_3$-only regime were predicted using a kinetic model (see Sect. 2.3) with different $k_{NO_3+CI}/k_{NO_3+OH}$ ratios. Figure 3 shows a measurement–model comparison of those signal ratios. When the ratio of $k_{NO_3+CI}/k_{NO_3+OH}$ is smaller than or equal to 1, the simulated signal ratios of a large amount of $RO_2$ and HOMs differ significantly from the measured ratios, especially for some $C_{10}H_{17}O_x$ $RO_2$ and $C_{10}H_{18}O_x$ HOMs. When the ratio of $k_{NO_3+CI}/k_{NO_3+OH}$ is 10–100, there is a good measurement–model agreement for most of the $RO_2$ and HOMs. Therefore, we conclude that the cross-reaction rate constants of $^{NO_3}RO_2 + {}^{CI}RO_2$ are on average 10–100 times larger than those for $^{NO_3}RO_2 + {}^{OH}RO_2$. This different $RO_2$ cross-reaction efficiency is the main reason for the significantly larger decrease in the abundance of $^{CI}RO_2$ and related HOMs as compared to the OH-derived ones (see Fig. 2).

As a competitive reaction pathway, the autoxidation rates of $RO_2$ can affect the extent to which $RO_2$ cross reactions influence the $RO_2$ fate and HOM formation. Therefore, sensitivity analyses of the autoxidation rate of $RO_2$ were conducted to evaluate its influence on the changes in $RO_2$ and related HOM concentrations in the synergistic $O_3 + NO_3$ regime vs. the $O_3$-only regime (Fig. S6). In these analyses, a $k_{NO_3+CI}/k_{NO_3+OH}$ ratio of 10 was used according to the above discussions. As the autoxidation rate of $^{OH}RO_2$ increases from 0.28 to 10 $s^{-1}$, corresponding to the rate range reported in previous studies (Berndt et al., 2016; Zhao et al., 2018; Xu et al., 2019), the simulated reduction in highly oxygenated $^{OH}RO_2$ and related $C_{10}H_{18}O_x$ HOMs in the synergistic $O_3 + NO_3$ regime exhibits a slight decrease (< 10 %) but still agrees reasonably well with the measured value (Fig. S6a–d). Considering that the autoxidation rates of $^{CI}RO_2$ used in the model approach their upper limits reported in the literature, i.e., $\sim 1\ s^{-1}$ for the butyl ring-opened $C_{10}H_{15}O_4$ $RO_2$ (Iyer et al., 2021) and relatively smaller rates for ring-retained $C_{10}H_{15}O_4$ $RO_2$ (0.02–0.29 $s^{-1}$; see Scheme S1 in the Supplement) (Zhao et al., 2021), we also lowered the autoxidation rate constants of $^{CI}RO_2$ by a factor of 10 to see its influence on $RO_2$ and HOM distribution in the $O_3 + NO_3$ regime. The simulated reduction in $^{CI}RO_2$ and $C_{10}H_{14}O_x$ HOMs in this case decreases by 7 %–16 % (Fig. S6e–h), while that of $C_{10}H_{16}O_x$ HOMs increases by up to 31 % (Fig. S6i and j). However, the simulated results are still close to the measured values. These sensitivity analyses suggest that the uncertainty in the autoxidation rates of $^{OH}RO_2$ and $^{CI}RO_2$ could slightly affect the simulated distribution of $RO_2$ and HOMs across different oxidation regimes but not significantly change the $k_{NO_3+CI}/k_{NO_3+OH}$ ratio obtained in this study. Further sensitivity analyses on the rate constant and dimer formation branching ratio of $RO_2$ cross reactions indicate that the uncertainties in these reaction kinetics do not alter the conclusion regarding the $k_{NO_3+CI}/k_{NO_3+OH}$ ratio either (see details in Sects. S2 and S3).

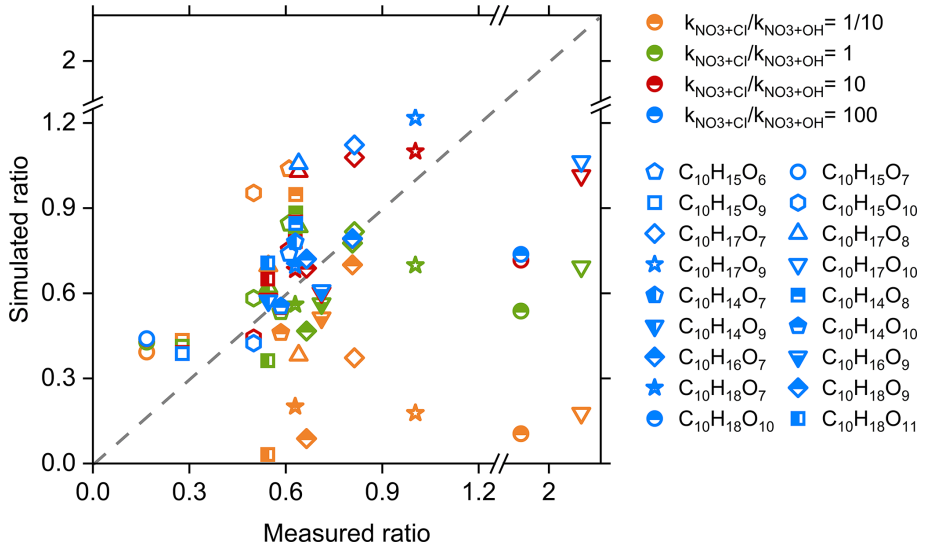


**Figure 3.** Measurement–model comparisons of the signal ratios of different $C_{10}$ $RO_2$ and HOMs in the synergistic $O_3 + NO_3$ regime vs. the $O_3$-only regime. The cross-reaction rate constant of $^{NO_3}RO_2 + {}^{Cl}RO_2$ was set to $2 \times 10^{-12}$ cm$^3$ molec.$^{-1}$ s$^{-1}$, and the rate of $^{NO_3}RO_2 + {}^{OH}RO_2$ was varied from $2 \times 10^{-11}$ to $2 \times 10^{-14}$ cm$^3$ molec.$^{-1}$ s$^{-1}$ in the model.

Cyclohexane was added in some experiments as an OH scavenger to elucidate the role of $^{OH}RO_2$ chemistry in HOM formation in the $O_3 + NO_3$ regime. In the presence of cyclohexane, most of the $^{OH}RO_2$ ($C_{10}H_{17}O_x$) and related HOM monomers ($C_{10}H_{18}O_x$) and dimers ($C_{20}H_{32}O_x$ and $C_{20}H_{34}O_x$) decrease by more than 70 % (Fig. 4), while $^{Cl}RO_2$ ($C_{10}H_{15}O_x$) and related HOM monomers ($C_{10}H_{14}O_x$) only decrease slightly. Accordingly, the reduction in $C_{20}H_{32}O_x$ and $C_{20}H_{34}O_x$ dimers is significantly larger than that of $C_{20}H_{30}O_x$. These results are in a good agreement with previous measurements (Zhao et al., 2018; Zang et al., 2023). The $C_{10}H_{16}O_x$ species, which can arise from both $^{Cl}RO_2$ and $^{OH}RO_2$, exhibit a medium reduction (Fig. 4b). It is interesting to note that with the addition of cyclohexane, there is a significant increase in $C_{20}H_{31}NO_x$, which is formed from the cross reactions of $^{Cl}RO_2$ with $^{NO_3}RO_2$. Such an enhanced production of $C_{20}H_{31}NO_x$ as compared to the slightly deceased formation of $C_{20}H_{30}O_x$ indicates that the $^{Cl}RO_2 + {}^{NO_3}RO_2$ reactions are competitive compared to the $^{Cl}RO_2 + {}^{Cl}RO_2$ and $^{Cl}RO_2 + {}^{OH}RO_2$ reactions. As a result, when the $^{OH}RO_2$ is depleted, the $^{Cl}RO_2$ that is supposed to react with $^{OH}RO_2$ efficiently reacts with $^{NO_3}RO_2$ to form $C_{20}H_{31}NO_x$, leading to the increase in $C_{20}H_{31}NO_x$ signals. Consistent with the experimental measurements, the model simulations show that the concentrations of $C_{20}H_{31}NO_x$ in the $O_3 + NO_3$ regime increase with the addition of cyclohexane as an OH scavenger (Fig. S9). However, the simulated enhancement is slightly lower than the measurements, which might be due to the uncertainties in the $RO_2$ cross-reaction kinetics in the model.

### 3.3 Influence of synergistic oxidation on low-volatility organics and particle formation

Compared to the $O_3$-only regime, there are a remarkable reduction in $C_xH_yO_z$ HOMs and a strong formation of HOM ONs due to the efficient cross reactions between $^{NO_3}RO_2$ and $^{Cl}RO_2$ in the synergistic-oxidation regime. This significant change in HOM composition and abundance would alter the volatility distribution of HOMs and influence the formation of particles. The volatilities of HOMs formed in the two oxidation regimes are estimated using a modified composition-activity method (see Sect. 2.2) and shown in Fig. 5. The abundance of $C_xH_yO_z$ HOMs characterized as ULVOCs and ELVOCs decreases considerably in the synergistic $O_3 + NO_3$ regime compared to the $O_3$-only regime (Fig. 5), in agreement with the very recent observations by Li et al. (2024), who found that the presence of $NO_3$ radicals during $\alpha$-pinene ozonolysis significantly reduced the abundance of ULVOCs. Although a substantial number of HOM ONs are formed in the $O_3 + NO_3$ regime, they generally have higher volatilities (i.e., characterized as ELVOCs to IVOCs) (Fig. 5). Therefore, the synergistic $O_3 + NO_3$ oxidation of $\alpha$-pinene significantly reduces the formation of ULVOCs and increases the overall volatility of total HOMs.

Figure 6a shows the particle number and mass concentrations formed in the two oxidation regimes in SOA formation experiments (experiments 13 and 14). The particle number concentration decreases by $\sim$ 50 %, whereas the particle mass concentration increases by a factor of 2 in the synergistic $O_3 + NO_3$ regime, compared to that in the $O_3$-only regime. The presence of $NO_3$ radicals during $\alpha$-pinene ozonolysis reduces the abundance of ULVOCs, which are the key species driving particle nucleation, thereby leading

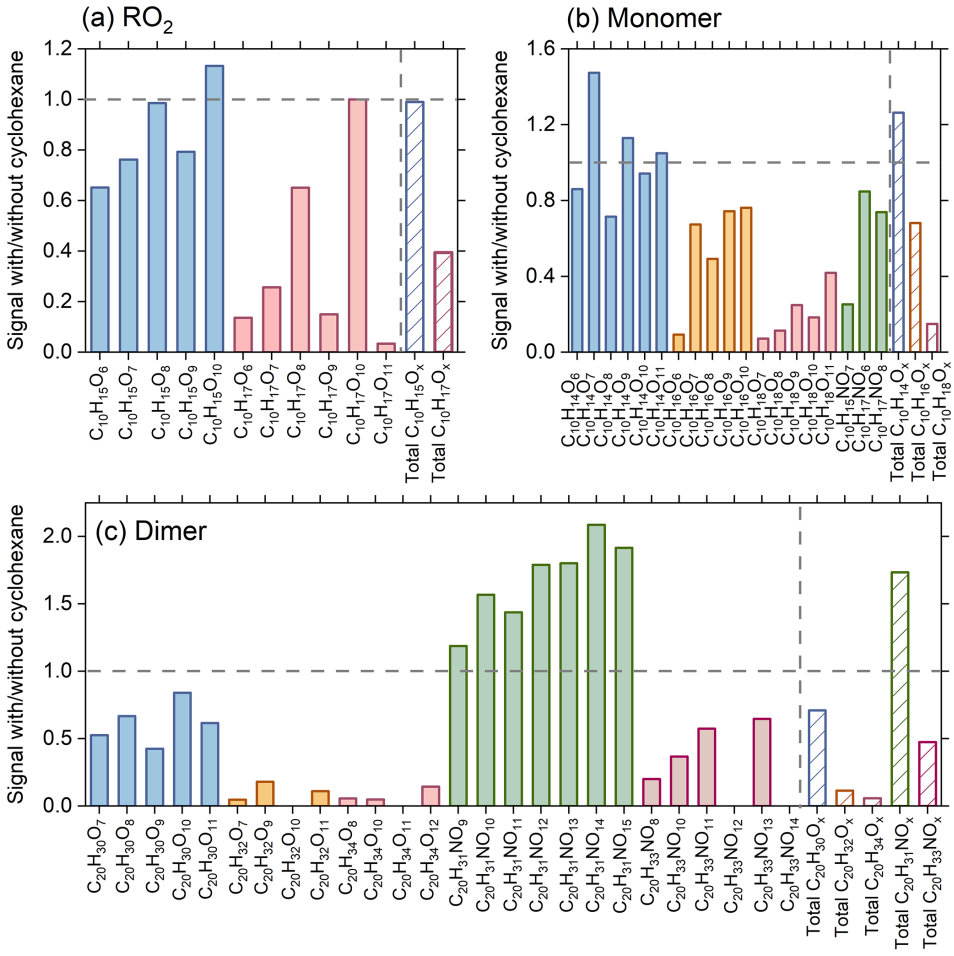


**Figure 4.** Relative changes in signals of **(a)** $C_{10}$ $RO_2$, **(b)** $C_{10}$ HOMs, and **(c)** $C_{20}$ dimers due to the addition of 100 ppm cyclohexane as an OH scavenger derived in the synergistic $O_3 + NO_3$ regime (experiments 6 and 12).

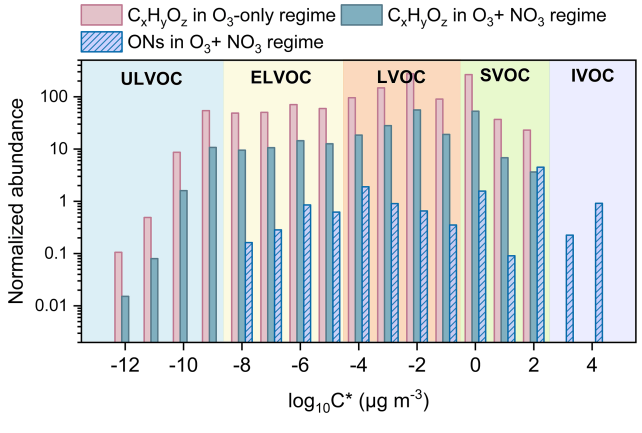


**Figure 5.** Volatility distribution of $C_xH_yO_z$ HOMs and HOM ONs formed in the $O_3 + NO_3$ regime and $O_3$-only regime (experiments 1 and 7). Ion signals in each oxidation regime are normalized to the corresponding total reacted $\alpha$-pinene.

to a reduction in the particle number concentration in the $O_3 + NO_3$ regime. On the other hand, substantial formation of HOM ONs is expected from the cross reactions of $^{NO_3}RO_2$ with $^{Cl}RO_2$ and $^{OH}RO_2$ in the synergistic-oxidation regime (Li et al., 2024; Bates et al., 2022), although their signals are relatively low due to the low sensitivity of nitrate CIMS to ONs in this study. The newly formed HOM ONs have relatively higher volatilities and are inefficient in initiating particle nucleation, but they are able to partition into the formed particles and contribute to the particle mass growth. Meanwhile, as the particle number concentration decreases drastically in the synergistic-oxidation regime, more condensable vapors are available for each particle to grow to larger sizes (Fig. 6b), which would in turn favor the condensation of more volatile organic species including ONs due to the reduced curvature effect of the larger particles, ultimately resulting in an increase in SOA mass concentrations.

Recently, Bates et al. (2022) also found that in chamber experiments with seed particles, the SOA mass yields were significantly higher during $\alpha$-pinene oxidation by $O_3 + NO_3$

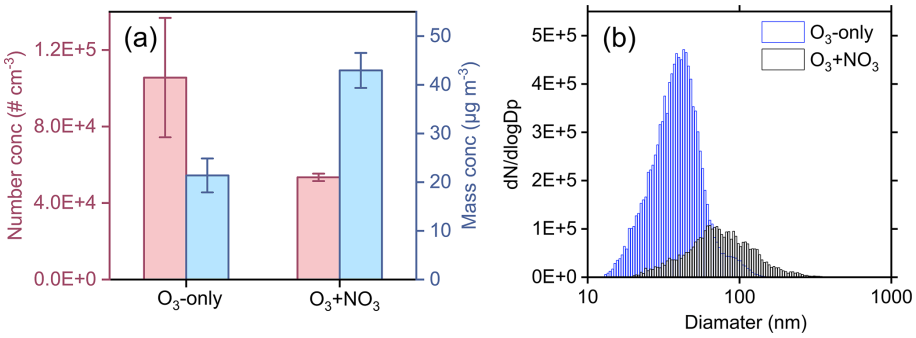


**Figure 6.** **(a)** Number and mass concentrations, as well as **(b)** the size distribution of particles formed from the ozonolysis and synergistic $O_3 + NO_3$ oxidation of $\alpha$-pinene (experiments 13 and 14).

than during ozonolysis, mainly due to the substantial formation and condensation of dimeric ONs. However, in the absence of seed particles, synergistic $O_3 + NO_3$ oxidation of $\alpha$-pinene does not nucleate in their study. This phenomenon might be due to the high concentrations of $NO_2$ (72 ppb) and $O_3$ (102 ppb) as well as the relatively low concentration of $\alpha$-pinene (27 ppb) in their experiments. As indicated by Bates et al. (2022), under these conditions $NO_3$ radicals were substantially formed and contributed to a dominant fraction (75 %) of $\alpha$-pinene oxidation, which strongly inhibited the production of low-volatility species and particle nucleation.

### 3.4 Atmospheric relevance of experimental results

In the present study, the flow tube experiments were conducted under dry conditions. Although water vapor may affect the fate of Criegee intermediates and $RO_2$ radicals and thereby HOM formation during the oxidation of organics under humid conditions, there is growing evidence that such effects in the $\alpha$-pinene oxidation system are small. Kinetic studies have found that the stabilized Criegee intermediates (SCIs) arising from $\alpha$-pinene ozonolysis can undergo fast unimolecular decay at a rate constant of 60–250 $s^{-1}$ (Vereecken et al., 2017; Newland et al., 2018), which is rapid compared to their reaction with water vapor, in particular for *syn*-SCIs, under atmospheric conditions (Vereecken et al., 2017; Newland et al., 2018). In addition, the yield of OH radicals from Criegee decomposition is independent of RH (Atkinson et al., 1992; Aschmann et al., 2002). Consistent with the fast unimolecular reaction kinetics revealed by these studies, recent laboratory measurements have shown that the contribution of SCIs to the formation of gas-phase and particle-phase dimers is small (< 20 %) during $\alpha$-pinene ozonolysis (Zhao et al., 2018, 2022). Furthermore, the molecular composition and abundance of HOM monomers and dimers (Li et al., 2019) and the formation of particle-phase dimers (Zhang et al., 2015; Kenseth et al., 2018) do not change significantly with RH ranging from 3 % to 92 %. These studies suggest that the humidity condition does not strongly affect the HOM formation chemistry in the $\alpha$-pinene ozonolysis system.

To evaluate the relevance of our experimental findings to the real atmosphere, we performed chemical model simulations of HOM formation from nocturnal synergistic $O_3 + NO_3$ oxidation of $\alpha$-pinene under typical atmospheric conditions. In these simulations, constant concentrations of $\alpha$-pinene (1 ppb), $O_3$ (30 ppb), NO (5 ppt), $NO_2$ (1.8 ppb), $NO_3$ radicals (0.2 or 1 ppt), OH radicals (5–$50 \times 10^4$ molecules $cm^{-3}$), and $HO_2$ radicals (4 ppt), as well as a constant RH of 50 % and temperature of 298 K were used as typical nocturnal conditions in the boreal forest according to the field studies (Stone et al., 2012; Lee et al., 2016; Brown and Stutz, 2012; Geyer et al., 2003; Kristensen et al., 2016; Hakola et al., 2012; Liebmann et al., 2018). Considering the rapid deposition of oxidized biogenic compounds (Nguyen et al., 2015), a typical dilution lifetime of 5 h (i.e., $k_{dil} = 1/5\,h^{-1}$) was assumed in the model. According to the above analysis, the cross-reaction rate constants for $^{NO_3}RO_2 + {}^{CI}RO_2$ and $^{NO_3}RO_2 + {}^{OH}RO_2$ were set to $2 \times 10^{-12}$ and $2 \times 10^{-13}$ $cm^3$ molec.$^{-1}$ $s^{-1}$ in the model, respectively. The formation of $RO_2$ with oxygen numbers higher than 11 was not considered in the model, due to the large uncertainty in the autoxidation rate constants of the highly oxygenated $RO_2$. In fact, the autoxidation rate of the highly oxygenated $RO_2$ is expected to be small given the significant decrease in the number of active sites for intramolecular H abstraction in the molecule. As a result, the contribution of the most oxygenated HOMs to the total HOM monomers could be relatively small (Zhao et al., 2018; Claflin et al., 2018).

In the absence of $NO_3$ radicals (with $NO_3$ concentrations and formation rates set to zero), the amount of $\alpha$-pinene consumed during 4 h of simulation is 1.04 ppb. When a relatively low $NO_3$ concentration (0.2 ppt) is considered (Fig. 7a), the amount of $\alpha$-pinene consumed is 1.48 ppb, and the ozonolysis is the primary loss pathway of $\alpha$-pinene (68 %), followed by $NO_3$ (30 %) and OH oxidation (2 %). The reactions of $RO_2 + HO_2$, $RO_2 + NO$, and $RO_2 + RO_2$ account for ~ 49 %, ~ 27 %, and ~ 24 % of the total $RO_2$ fate, respec-

tively (Fig. S10a). Compared to the ozonolysis of $\alpha$-pinene, the synergistic $O_3 + NO_3$ oxidation leads to a reduction of 3 % and 13 % in the formation of $C_xH_yO_z$ HOM monomers and dimers, respectively (Fig. 7b). Given that the concentrations of $\alpha$-pinene and oxidants were held constant during the simulation, the consumptions of $\alpha$-pinene by $O_3$ and OH radicals are the same across different oxidation regimes. Therefore, the decreases in the concentrations of $C_xH_yO_z$ HOM monomers and dimers in the presence of $NO_3$ oxidation are mainly due to the cross reactions of $^{NO_3}RO_2$ with other $RO_2$. When the $NO_3$ concentration is as high as 1 ppt as reported in field studies (Liebmann et al., 2018), the consumption of $\alpha$-pinene reaches 3.24 ppb, of which 68 % is contributed by $NO_3$ oxidation (Fig. 7c). Under this condition, the $RO_2 + RO_2$ reactions account for ~ 34 % of the total $RO_2$ fate (Fig. S10b). As a result, the cross reactions of $^{NO_3}RO_2$ with other $RO_2$ play a more important role in the HOM formation. The production of $C_xH_yO_z$ HOM monomers and dimers decreases by 12 % and 43 %, respectively, due to the presence of $NO_3$ oxidation (Fig. 7d). We note that the variation in RH from 0 %–90 % in the model has negligible influence on the relative changes in $C_xH_yO_z$ HOMs under these nocturnal atmospheric conditions (Fig. S11). Considering that there are uncertainties in the dilution rate constant, a sensitivity analysis was performed by varying the $k_{dil}$ in the range of 0.04–0.2 $h^{-1}$. It is found that the variation within these rate values does not significantly influence the response of $C_xH_yO_z$ HOM dimer formation to concurrent $NO_3$ oxidation (Fig. S12).

Field observations have shown that $NO_3$ radicals, $O_3$, and OH radicals all had important contributions to monoterpene oxidation during the early morning after sunrise and late afternoon before sunset in the southeastern United States (Zhang et al., 2018). In addition, relatively high nighttime OH concentrations of $(2–10) \times 10^5$ molecules $cm^{-3}$ were measured in some areas such as Germany and New York City (Faloona et al., 2001; Geyer et al., 2003). As a result, a model simulation was conducted using OH concentration that was 10 times higher ($5 \times 10^5$ molecules $cm^{-3}$). The concentration of $NO_3$ radicals is 1 ppt, and the concentrations of other species are the same as the values mentioned above. With a higher OH concentration, $O_3$, $NO_3$, and OH radicals account for 28 %, 61 %, and 11 % to the total $\alpha$-pinene consumption, respectively (Fig. S13a). Compared to the results under low OH concentration, the formation of $C_xH_yO_z$ HOM monomers and dimers are all enhanced under high OH concentration (Fig. S13b). This is mainly due to the promoted self-reactions/cross reactions of $^{OH}RO_2$, as well as the promoted formation of $C_{10}H_{15}O_x$ $RO_2$ derived from the H-abstraction pathway by OH radicals. Nevertheless, the presence of $NO_3$ oxidation still reduces the formation of $C_xH_yO_z$ HOM dimers by 26 % (Fig. S13b).

Furthermore, model simulations under typical conditions in the southeastern United States (see details in Sect. S4) suggest that the coexistence of isoprene appears to exacerbate the suppression effect of synergistic oxidation on HOM formation from monoterpenes. As shown in Fig. S14, in the absence of isoprene, the synergistic $O_3 + NO_3$ oxidation of $\alpha$-pinene leads to a reduction of 13 % and 24 % in the formation of $C_xH_yO_z$ HOM monomers and dimers, respectively. When isoprene is present, as the isoprene + $NO_3$ oxidation produces a significant amount of nitrooxy $RO_2$ that can also scavenge $\alpha$-pinene-derived $^{CI}RO_2$ and $^{OH}RO_2$ via cross reactions, the synergistic oxidation leads to a slightly larger reduction in $C_xH_yO_z$ HOM monomers and dimers (15 % and 31 %, respectively).

The above model simulations suggest that under nocturnal atmospheric conditions with a very low $NO_3$ concentration, the $RO_2$ radical pool is dominated by $^{CI}RO_2$ and the self-reactions/cross reactions of which are a major contributor to ULVOCs such as the highly oxygenated $C_{20}$ dimers as observed in boreal forest (Bianchi et al., 2017). When the $NO_3$ concentration is high, the production of $^{NO_3}RO_2$ becomes significant and the cross reactions of which with $^{CI}RO_2$ would suppress the formation of ULVOCs. Although HOM ON dimers are readily produced by cross reactions between $^{NO_3}RO_2$ and $^{CI}RO_2$, they generally have higher volatilities than $C_xH_yO_z$ HOM dimers and therefore are less efficient in initiating particle formation. However, these HOM ONs can be an important contributor to the particle mass growth. As suggested by the model simulations in Bates et al. (2022), the $NO_3$ oxidation of $\alpha$-pinene led to a partic-

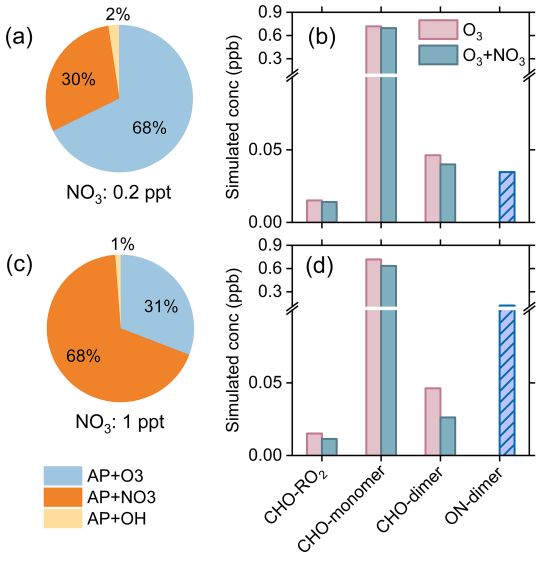


**Figure 7.** Model simulations of $\alpha$-pinene (AP) oxidation and HOM formation under typical nighttime conditions in the boreal forest. **(a, c)** Contributions of different loss pathways of $\alpha$-pinene by different oxidants at $NO_3$ concentrations of 0.2 and 1 ppt, respectively. **(b, d)** Concentrations of $C_xH_yO_z$ HOMs and HOM ONs formed by synergistic $O_3 + NO_3$ oxidation and ozonolysis of $\alpha$-pinene under conditions corresponding to **(a)** and **(c)**. The simulations were run for 4 h after an 8 h spin-up for intermediates and secondary species.

ulate nitrate yield of 7 % under nocturnal atmospheric conditions in rural Alabama during the Southern Oxidant and Aerosol Study (SOAS) campaign. Our results offer mechanistic and quantitative insights into how the synergistic oxidation of $\alpha$-pinene by $O_3$ and $NO_3$ radicals can influence the formation of low-volatility organic compounds and hence particle formation and growth. They also provide a potential explanation for field observations regarding NPF events frequently occurring in monoterpene-rich regions during daytime but not at nighttime (Mohr et al., 2017; Kulmala et al., 2001; Junninen et al., 2017).

## 4 Conclusions

This study provides a comprehensive characterization of the nocturnal synergistic oxidation of $\alpha$-pinene by $O_3$ and $NO_3$ radicals and its influence on the formation of HOMs and low-volatility organic compounds using a combination of flow reactor experiments and detailed kinetic model simulations. It is found that the formation of $C_xH_yO_z$ HOMs in the $O_3 + NO_3$ regime is significantly suppressed compared to that in the $O_3$-only regime, mainly due to the depletion of ozonolysis-derived $RO_2$ (i.e., $^{CI}RO_2$ and $^{OH}RO_2$) by $^{NO_3}RO_2$ via cross reactions. In addition, the decreases in the abundance of $^{CI}RO_2$ and related HOMs are significantly larger than those of OH-derived ones, indicating that the $^{NO_3}RO_2$ species react more efficiently with $^{CI}RO_2$ than with $^{OH}RO_2$. Detailed measurement–model comparisons for the distribution of a suite of $^{CI}RO_2$, $^{OH}RO_2$, and associated HOMs across different oxidation regimes further reveal that the cross reactions between $^{CI}RO_2$ and $^{NO_3}RO_2$ are on average 10–100 times more efficient than those of $^{OH}RO_2$ and $^{NO_3}RO_2$.

The suppressed formation of $C_xH_yO_z$ HOMs in the synergistic $O_3 + NO_3$ regime results in a significant reduction in ULVOCs. Although a substantial number of HOM ONs are formed from the cross reactions between $^{NO_3}RO_2$ and $^{CI}RO_2$ or $^{OH}RO_2$ in the synergistic-oxidation regime, they have higher volatilities and are less likely to participate in the formation and initial growth of new particles. As a result, in our experiment the formation of new particles in the synergistic-oxidation regime is substantially inhibited compared to the $O_3$-only regime. Chemical model simulations further confirm that the synergistic oxidation of $\alpha$-pinene by $O_3$ and $NO_3$ radicals can significantly inhibit the formation of $C_xH_yO_z$ HOMs, especially the ultralow-volatility $C_xH_yO_z$ HOM dimers under typical nighttime atmospheric conditions. Our study sheds lights on the synergistic-oxidation mechanism of biogenic emissions and underscores the importance of considering this chemistry for a better depiction of the formation of low-volatility organics and particles in the atmosphere.

**Code and data availability.** The data presented in this work are available upon request from the corresponding author. The code of F0AM v4.1 is available at https://github.com/AirChem/F0AM.git (Wolfe, 2024).

**Supplement.** The supplement related to this article is available online at: https://doi.org/10.5194/acp-24-11701-2024-supplement.

**Author contributions.** YZ and HZ designed the study, and HZ and DH performed the experiments. YZ and HZ analyzed the data, conducted model simulations, and wrote the paper. All other authors contributed to discussion and writing.

**Competing interests.** The contact author has declared that none of the authors has any competing interests.

**Disclaimer.** Publisher's note: Copernicus Publications remains neutral with regard to jurisdictional claims made in the text, published maps, institutional affiliations, or any other geographical representation in this paper. While Copernicus Publications makes every effort to include appropriate place names, the final responsibility lies with the authors.

**Acknowledgements.** We gratefully acknowledge the financial support of the National Natural Science Foundation of China (grant nos. 22376137 and 22022607) and the Science and Technology Commission of Shanghai Municipality (grant no. 21230711000).

**Financial support.** This research has been supported by the National Natural Science Foundation of China (grant nos. 22376137 and 22022607) and the Science and Technology Commission of Shanghai Municipality (grant no. 21230711000).

**Review statement.** This paper was edited by Kelvin Bates and reviewed by three anonymous referees.

## References

Aschmann, S. M., Arey, J., and Atkinson, R.: OH radical formation from the gas-phase reactions of $O_3$ with a series of terpenes, Atmos. Environ., 36, 4347–4355, https://doi.org/10.1016/S1352-2310(02)00355-2, 2002.

Atkinson, R., Aschmann, S. M., Arey, J., and Shorees, B.: Formation of OH radicals in the gas-phase reactions of $O_3$ with a series of terpenes, J. Geophys. Res.-Atmos., 97, 6065–6073, https://doi.org/10.1029/92JD00062, 1992.

Bates, K. H., Burke, G. J. P., Cope, J. D., and Nguyen, T. B.: Secondary organic aerosol and organic nitrogen yields from the nitrate radical ($NO_3$) oxidation of alpha-pinene from

various $RO_2$ fates, Atmos. Chem. Phys., 22, 1467–1482, https://doi.org/10.5194/acp-22-1467-2022, 2022.

Berndt, T.: Peroxy radical processes and product formation in the OH radical-initiated oxidation of alpha-pinene for near-atmospheric conditions, J. Phys. Chem. A, 125, 9151–9160, https://doi.org/10.1021/acs.jpca.1c05576, 2021.

Berndt, T., Richters, S., Jokinen, T., Hyttinen, N., Kurtén, T., Otkjær, R. V., Kjaergaard, H. G., Stratmann, F., Herrmann, H., Sipilä, M., Kulmala, M., and Ehn, M.: Hydroxyl radical-induced formation of highly oxidized organic compounds, Nat. Commun., 7, 13677, https://doi.org/10.1038/ncomms13677, 2016.

Berndt, T., Mentler, B., Scholz, W., Fischer, L., Herrmann, H., Kulmala, M., and Hansel, A.: Accretion product formation from ozonolysis and OH radical reaction of $\alpha$-pinene: mechanistic insight and the influence of isoprene and ethylene, Environ. Sci. Technol., 52, 11069–11077, https://doi.org/10.1021/acs.est.8b02210, 2018.

Bianchi, F., Garmash, O., He, X., Yan, C., Iyer, S., Rosendahl, I., Xu, Z., Rissanen, M. P., Riva, M., Taipale, R., Sarnela, N., Petäjä, T., Worsnop, D. R., Kulmala, M., Ehn, M., and Junninen, H.: The role of highly oxygenated molecules (HOMs) in determining the composition of ambient ions in the boreal forest, Atmos. Chem. Phys., 17, 13819–13831, https://doi.org/10.5194/acp-17-13819-2017, 2017.

Bianchi, F., Kurtén, T., Riva, M., Mohr, C., Rissanen, M. P., Roldin, P., Berndt, T., Crounse, J. D., Wennberg, P. O., Mentel, T. F., Wildt, J., Junninen, H., Jokinen, T., Kulmala, M., Worsnop, D. R., Thornton, J. A., Donahue, N., Kjaergaard, H. G., and Ehn, M.: Highly oxygenated organic molecules (HOM) from gas-phase autoxidation involving peroxy radicals: a key contributor to atmospheric aerosol, Chem. Rev., 119, 3472–3509, https://doi.org/10.1021/acs.chemrev.8b00395, 2019.

Boyd, C. M., Sanchez, J., Xu, L., Eugene, A. J., Nah, T., Tuet, W. Y., Guzman, M. I., and Ng, N. L.: Secondary organic aerosol formation from the $\beta$-pinene + $NO_3$ system: effect of humidity and peroxy radical fate, Atmos. Chem. Phys., 15, 7497–7522, https://doi.org/10.5194/acp-15-7497-2015, 2015.

Brown, S. S. and Stutz, J.: Nighttime radical observations and chemistry, Chem. Soc. Rev., 41, 6405–6447, https://doi.org/10.1039/c2cs35181a, 2012.

Claflin, M. S., Krechmer, J. E., Hu, W., Jimenez, J. L., and Ziemann, P. J.: Functional group composition of secondary organic aerosol formed from ozonolysis of $\alpha$-pinene under high VOC and autoxidation conditions, ACS Earth Space Chem., 2, 1196–1210, https://doi.org/10.1021/acsearthspacechem.8b00117, 2018.

Daumit, K. E., Kessler, S. H., and Kroll, J. H.: Average chemical properties and potential formation pathways of highly oxidized organic aerosol, Faraday Discuss., 165, 181–202, https://doi.org/10.1039/c3fd00045a, 2013.

Donahue, N. M., Epstein, S. A., Pandis, S. N., and Robinson, A. L.: A two-dimensional volatility basis set: 1. organic-aerosol mixing thermodynamics, Atmos. Chem. Phys., 11, 3303–3318, https://doi.org/10.5194/acp-11-3303-2011, 2011.

Donahue, N. M., Henry, K. M., Mentel, T. F., Kiendler-Scharr, A., Spindler, C., Bohn, B., Brauers, T., Dorn, H. P., Fuchs, H., Tillmann, R., Wahner, A., Saathoff, H., Naumann, K.-H., Möhler, O., Leisner, T., Müller, L., Reinnig, M.-C., Hoffmann, T., Salo, K., Hallquist, M., Frosch, M., Bilde, M., Tritscher, T., Barmet, P., Praplan, A. P., DeCarlo, P. F., Dommen, J., Prévôt, A. S. H., and Baltensperger, U.: Aging of biogenic secondary organic aerosol via gas-phase OH radical reactions, P. Natl. Acad. Sci. USA, 109, 13503–13508, https://doi.org/10.1073/pnas.1115186109, 2012.

Ehn, M., Thornton, J. A., Kleist, E., Sipilä, M., Junninen, H., Pullinen, I., Springer, M., Rubach, F., Tillmann, R., and Lee, B.: A large source of low-volatility secondary organic aerosol, Nature, 506, 476–479, https://doi.org/10.1038/nature13032, 2014.

Faloona, I., Tan, D., Brune, W., Hurst, J., Barket, D., Couch, T. L., Shepson, P., Apel, E., Riemer, D., Thornberry, T., Carroll, M. A., Sillman, S., Keeler, G. J., Sagady, J., Hooper, D., and Paterson, K.: Nighttime observations of anomalously high levels of hydroxyl radicals above a deciduous forest canopy, J. Geophys. Res.-Atmos., 106, 24315–24333, https://doi.org/10.1029/2000JD900691, 2001.

Fry, J. L., Draper, D. C., Barsanti, K. C., Smith, J. N., Ortega, J., Winkler, P. M., Lawler, M. J., Brown, S. S., Edwards, P. M., Cohen, R. C., and Lee, L.: Secondary organic aerosol formation and organic nitrate yield from $NO_3$ oxidation of biogenic hydrocarbons, Environ. Sci. Technol., 48, 11944–11953, https://doi.org/10.1021/es502204x, 2014.

Geyer, A., Bächmann, K., Hofzumahaus, A., Holland, F., Konrad, S., Klüpfel, T., Pätz, H. W., Perner, D., Mihelcic, D., Schäfer, H. J., Volz-Thomas, A., and Platt, U.: Nighttime formation of peroxy and hydroxyl radicals during the BERLIOZ campaign: Observations and modeling studies, J. Geophys. Res.-Atmos., 108, 8249, https://doi.org/10.1029/2001JD000656, 2003.

Hakola, H., Hellén, H., Hemmilä, M., Rinne, J., and Kulmala, M.: In situ measurements of volatile organic compounds in a boreal forest, Atmos. Chem. Phys., 12, 11665–11678, https://doi.org/10.5194/acp-12-11665-2012, 2012.

Hallquist, M., Wängberg, I., Ljungström, E., Barnes, I., and Becker, K. H.: Aerosol and product yields from $NO_3$ radical-initiated oxidation of selected monoterpenes, Environ. Sci. Technol., 33, 553–559, https://doi.org/10.1021/es980292s, 1999.

Huang, R. J., Zhang, Y., Bozzetti, C., Ho, K. F., Cao, J. J., Han, Y., Daellenbach, K. R., Slowik, J. G., Platt, S. M., Canonaco, F., Zotter, P., Wolf, R., Pieber, S. M., Bruns, E. A., Crippa, M., Ciarelli, G., Piazzalunga, A., Schwikowski, M., Abbaszade, G., Schnelle-Kreis, J., Zimmermann, R., An, Z., Szidat, S., Baltensperger, U., El Haddad, I., and Prevot, A. S.: High secondary aerosol contribution to particulate pollution during haze events in China, Nature, 514, 218–222, https://doi.org/10.1038/nature13774, 2014.

Huang, W., Saathoff, H., Shen, X., Ramisetty, R., Leisner, T., and Mohr, C.: Chemical characterization of highly functionalized organonitrates contributing to night-time organic aerosol mass loadings and particle growth, Environ. Sci. Technol., 53, 1165–1174, https://doi.org/10.1021/acs.est.8b05826, 2019.

Hyttinen, N., Kupiainen-Määttä, O., Rissanen, M. P., Muuronen, M., Ehn, M., and Kurtén, T.: Modeling the charging of highly oxidized cyclohexene ozonolysis products using nitrate-based chemical ionization, J. Phys. Chem. A, 119, 6339–6345, https://doi.org/10.1021/acs.jpca.5b01818, 2015.

Inomata, S.: New particle formation promoted by OH reactions during $\alpha$-pinene ozonolysis, ACS Earth Space Chem., 5, 1929–1933, https://doi.org/10.1021/acsearthspacechem.1c00142, 2021.

Isaacman-VanWertz, G. and Aumont, B.: Impact of organic molecular structure on the estimation of atmospherically relevant

physicochemical parameters, Atmos. Chem. Phys., 21, 6541–6563, https://doi.org/10.5194/acp-21-6541-2021, 2021.

Iyer, S., Rissanen, M. P., Valiev, R., Barua, S., Krechmer, J. E., Thornton, J., Ehn, M., and Kurten, T.: Molecular mechanism for rapid autoxidation in alpha-pinene ozonolysis, Nat. Commun., 12, 878, https://doi.org/10.1038/s41467-021-21172-w, 2021.

Jenkin, M. E., Young, J. C., and Rickard, A. R.: The MCM v3.3.1 degradation scheme for isoprene, Atmos. Chem. Phys., 15, 11433–11459, https://doi.org/10.5194/acp-15-11433-2015, 2015.

Jokinen, T., Sipilä, M., Richters, S., Kerminen, V. M., Paasonen, P., Stratmann, F., Worsnop, D., Kulmala, M., Ehn, M., and Herrmann, H.: Rapid autoxidation forms highly oxidized $RO_2$ radicals in the atmosphere, Angew. Chem. Int. Edit., 53, 14596–14600, https://doi.org/10.1002/anie.201408566, 2014.

Junninen, H., Ehn, M., Petäjä, T., Luosujärvi, L., Kotiaho, T., Kostiainen, R., Rohner, U., Gonin, M., Fuhrer, K., Kulmala, M., and Worsnop, D. R.: A high-resolution mass spectrometer to measure atmospheric ion composition, Atmos. Meas. Tech., 3, 1039–1053, https://doi.org/10.5194/amt-3-1039-2010, 2010.

Junninen, H., Hulkkonen, M., Riipinen, I., Nieminen, T., Hirsikko, A., Suni, T., Boy, M., Lee, S.-H., Vana, M., Tammet, H., Kerminen, V.-M., and Kulmala, M.: Observations on nocturnal growth of atmospheric clusters, Tellus B, 60, 365–371, https://doi.org/10.1111/j.1600-0889.2008.00356.x, 2017.

Kenseth, C. M., Huang, Y., Zhao, R., Dalleska, N. F., Hethcox, J. C., Stoltz, B. M., and Seinfeld, J. H.: Synergistic $O_3$ + OH oxidation pathway to extremely low-volatility dimers revealed in beta-pinene secondary organic aerosol, P. Natl. Acad. Sci. USA, 115, 8301–8306, https://doi.org/10.1073/pnas.1804671115, 2018.

Kirkby, J., Duplissy, J., Sengupta, K., Frege, C., Gordon, H., Williamson, C., Heinritzi, M., Simon, M., Yan, C., Almeida, J., Tröstl, J., Nieminen, T., Ortega, I. K., Wagner, R., Adamov, A., Amorim, A., Bernhammer, A.-K., Bianchi, F., Breitenlechner, M., Brilke, S., Chen, X., Craven, J., Dias, A., Ehrhart, S., Flagan, R. C., Franchin, A., Fuchs, C., Guida, R., Hakala, J., Hoyle, C. R., Jokinen, T., Junninen, H., Kangasluoma, J., Kim, J., Krapf, M., Kürten, A., Laaksonen, A., Lehtipalo, K., Makhmutov, V., Mathot, S., Molteni, U., Onnela, A., Peräkylä, O., Piel, F., Petäjä, T., Praplan, A. P., Pringle, K., Rap, A., Richards, N. A. D., Riipinen, I., Rissanen, M. P., Rondo, L., Sarnela, N., Schobesberger, S., Scott, C. E., Seinfeld, J. H., Sipilä, M., Steiner, G., Stozhkov, Y., Stratmann, F., Tomé, A., Virtanen, A., Vogel, A. L., Wagner, A. C., Wagner, P. E., Weingartner, E., Wimmer, D., Winkler, P. M., Ye, P., Zhang, X., Hansel, A., Dommen, J., Donahue, N. M., Worsnop, D. R., Baltensperger, U., Kulmala, M., Carslaw, K. S., and Curtius, J.: Ion-induced nucleation of pure biogenic particles, Nature, 533, 521–526, https://doi.org/10.1038/nature17953, 2016.

Kristensen, K., Watne, Å. K., Hammes, J., Lutz, A., Petäjä, T., Hallquist, M., Bilde, M., and Glasius, M.: High-molecular weight dimer esters are major products in aerosols from $\alpha$-pinene ozonolysis and the boreal forest, Environ. Sci. Tech. Let., 3, 280–285, https://doi.org/10.1021/acs.estlett.6b00152, 2016.

Kulmala, M., Hämeri, K., Aalto, P. P., Mäkelä, J. M., Pirjola, L., Nilsson, E. D., Buzorius, G., Rannik, Ü., Dal Maso, M., Seidl, W., Hoffman, T., Janson, R., Hansson, H. C., Viisanen, Y., Laaksonen, A., and O'Dowd, C. D.: Overview of the international project on biogenic aerosol formation in the boreal forest (BIOFOR), Tellus B, 53, 324–343, https://doi.org/10.1034/j.1600-0889.2001.530402.x, 2001.

Kurtén, T., Møller, K. H., Nguyen, T. B., Schwantes, R. H., Misztal, P. K., Su, L., Wennberg, P. O., Fry, J. L., and Kjaergaard, H. G.: Alkoxy radical bond scissions explain the anomalously low secondary organic aerosol and organonitrate yields from $\alpha$-pinene + $NO_3$, J. Phys. Chem. Lett., 8, 2826–2834, https://doi.org/10.1021/acs.jpclett.7b01038, 2017.

Lee, B. H., D'Ambro, E. L., Lopez-Hilfiker, F. D., Schobesberger, S., Mohr, C., Zawadowicz, M. A., Liu, J., Shilling, J. E., Hu, W., Palm, B. B., Jimenez, J. L., Hao, L., Virtanen, A., Zhang, H., Goldstein, A. H., Pye, H. O. T., and Thornton, J. A.: Resolving ambient organic aerosol formation and aging pathways with simultaneous molecular composition and volatility observations, ACS Earth Space Chem., 4, 391–402, https://doi.org/10.1021/acsearthspacechem.9b00302, 2020.

Lee, S. H., Uin, J., Guenther, A. B., de Gouw, J. A., Yu, F. Q., Nadykto, A. B., Herb, J., Ng, N. L., Koss, A., Brune, W. H., Baumann, K., Kanawade, V. P., Keutsch, F. N., Nenes, A., Olsen, K., Goldstein, A., and Ouyang, Q.: Isoprene suppression of new particle formation: Potential mechanisms and implications, J. Geophys. Res.-Atmos., 121, 14621–14635, https://doi.org/10.1002/2016jd024844, 2016.

Li, D., Huang, W., Wang, D., Wang, M., Thornton, J. A., Caudillo, L., Rörup, B., Marten, R., Scholz, W., Finkenzeller, H., Marie, G., Baltensperger, U., Bell, D. M., Brasseur, Z., Curtius, J., Dada, L., Duplissy, J., Gong, X., Hansel, A., He, X.-C., Hofbauer, V., Junninen, H., Krechmer, J. E., Kürten, A., Lamkaddam, H., Lehtipalo, K., Lopez, B., Ma, Y., Mahfouz, N. G. A., Manninen, H. E., Mentler, B., Perrier, S., Petäjä, T., Pfeifer, J., Philippov, M., Schervish, M., Schobesberger, S., Shen, J., Surdu, M., Tomaz, S., Volkamer, R., Wang, X., Weber, S. K., Welti, A., Worsnop, D. R., Wu, Y., Yan, C., Zauner-Wieczorek, M., Kulmala, M., Kirkby, J., Donahue, N. M., George, C., El-Haddad, I., Bianchi, F., and Riva, M.: Nitrate radicals suppress biogenic new particle formation from monoterpene oxidation, Environ. Sci. Technol., 58, 1601–1614, https://doi.org/10.1021/acs.est.3c07958, 2024.

Li, X., Chee, S., Hao, J., Abbatt, J. P. D., Jiang, J., and Smith, J. N.: Relative humidity effect on the formation of highly oxidized molecules and new particles during monoterpene oxidation, Atmos. Chem. Phys., 19, 1555–1570, https://doi.org/10.5194/acp-19-1555-2019, 2019.

Li, Y., Pöschl, U., and Shiraiwa, M.: Molecular corridors and parameterizations of volatility in the chemical evolution of organic aerosols, Atmos. Chem. Phys., 16, 3327–3344, https://doi.org/10.5194/acp-16-3327-2016, 2016.

Liebmann, J., Karu, E., Sobanski, N., Schuladen, J., Ehn, M., Schallhart, S., Quéléver, L., Hellen, H., Hakola, H., Hoffmann, T., Williams, J., Fischer, H., Lelieveld, J., and Crowley, J. N.: Direct measurement of $NO_3$ radical reactivity in a boreal forest, Atmos. Chem. Phys., 18, 3799–3815, https://doi.org/10.5194/acp-18-3799-2018, 2018.

Liu, J., D'Ambro, E. L., Lee, B. H., Schobesberger, S., Bell, D. M., Zaveri, R. A., Zelenyuk, A., Thornton, J. A., and Shilling, J. E.: Monoterpene photooxidation in a continuous-flow chamber: SOA yields and impacts of oxidants, $NO_x$, and VOC precursors, Environ. Sci. Technol., 56, 12066–12076, https://doi.org/10.1021/acs.est.2c02630, 2022.

Martinez, E., Cabanas, B., Aranda, A., and Martin, P.: Kinetics of the reactions of $NO_3$ radical with selected monoterpenes: A temperature dependence study, Environ. Sci. Technol., 32, 3730–3734, https://doi.org/10.1021/es970899t, 1998.

Mentel, T. F., Springer, M., Ehn, M., Kleist, E., Pullinen, I., Kurtén, T., Rissanen, M., Wahner, A., and Wildt, J.: Formation of highly oxidized multifunctional compounds: autoxidation of peroxy radicals formed in the ozonolysis of alkenes – deduced from structure–product relationships, Atmos. Chem. Phys., 15, 6745–6765, https://doi.org/10.5194/acp-15-6745-2015, 2015.

Mohr, C., Lopez-Hilfiker, F. D., Yli-Juuti, T., Heitto, A., Lutz, A., Hallquist, M., D'Ambro, E. L., Rissanen, M. P., Hao, L., Schobesberger, S., Kulmala, M., Mauldin, R. L., Makkonen, U., Sipilä, M., Petäjä, T., and Thornton, J. A.: Ambient observations of dimers from terpene oxidation in the gas phase: Implications for new particle formation and growth, Geophys. Res. Lett., 44, 2958–2966, https://doi.org/10.1002/2017gl072718, 2017.

Molteni, U., Simon, M., Heinritzi, M., Hoyle, C. R., Bernhammer, A.-K., Bianchi, F., Breitenlechner, M., Brilke, S., Dias, A., Duplissy, J., Frege, C., Gordon, H., Heyn, C., Jokinen, T., Kürten, A., Lehtipalo, K., Makhmutov, V., Petäjä, T., Pieber, S. M., Praplan, A. P., Schobesberger, S., Steiner, G., Stozhkov, Y., Tomé, A., Tröstl, J., Wagner, A. C., Wagner, R., Williamson, C., Yan, C., Baltensperger, U., Curtius, J., Donahue, N. M., Hansel, A., Kirkby, J., Kulmala, M., Worsnop, D. R., and Dommen, J.: Formation of highly oxygenated organic molecules from $\alpha$-pinene ozonolysis: chemical characteristics, mechanism, and kinetic model development, ACS Earth Space Chem., 3, 873–883, https://doi.org/10.1021/acsearthspacechem.9b00035, 2019.

Mutzel, A., Zhang, Y., Böge, O., Rodigast, M., Kolodziejczyk, A., Wang, X., and Herrmann, H.: Importance of secondary organic aerosol formation of $\alpha$-pinene, limonene, and *m*-cresol comparing day- and nighttime radical chemistry, Atmos. Chem. Phys., 21, 8479–8498, https://doi.org/10.5194/acp-21-8479-2021, 2021.

Newland, M. J., Rickard, A. R., Sherwen, T., Evans, M. J., Vereecken, L., Muñoz, A., Ródenas, M., and Bloss, W. J.: The atmospheric impacts of monoterpene ozonolysis on global stabilised Criegee intermediate budgets and $SO_2$ oxidation: experiment, theory and modelling, Atmos. Chem. Phys., 18, 6095–6120, https://doi.org/10.5194/acp-18-6095-2018, 2018.

Nguyen, T. B., Crounse, J. D., Teng, A. P., St. Clair, J. M., Paulot, F., Wolfe, G. M., and Wennberg, P. O.: Rapid deposition of oxidized biogenic compounds to a temperate forest, P. Natl. Acad. Sci. USA, 112, E392–E401, https://doi.org/10.1073/pnas.1418702112, 2015.

Perraud, V., Bruns, E. A., Ezell, M. J., Johnson, S. N., Greaves, J., and Finlayson-Pitts, B. J.: Identification of organic nitrates in the $NO_3$ radical initiated oxidation of $\alpha$-pinene by atmospheric pressure chemical ionization mass spectrometry, Environ. Sci. Technol., 44, 5887–5893, https://doi.org/10.1021/es1005658, 2010.

Pye, H. O. T., Ward-Caviness, C. K., Murphy, B. N., Appel, K. W., and Seltzer, K. M.: Secondary organic aerosol association with cardiorespiratory disease mortality in the United States, Nat. Commun., 12, 7215, https://doi.org/10.1038/s41467-021-27484-1, 2021.

Schervish, M. and Donahue, N. M.: Peroxy radical chemistry and the volatility basis set, Atmos. Chem. Phys., 20, 1183–1199, https://doi.org/10.5194/acp-20-1183-2020, 2020.

Shen, H., Vereecken, L., Kang, S., Pullinen, I., Fuchs, H., Zhao, D., and Mentel, T. F.: Unexpected significance of a minor reaction pathway in daytime formation of biogenic highly oxygenated organic compounds, Sci. Adv., 8, eabp8702, https://doi.org/10.1126/sciadv.abp8702, 2022.

Shrivastava, M., Cappa, C. D., Fan, J., Goldstein, A. H., Guenther, A. B., Jimenez, J. L., Kuang, C., Laskin, A., Martin, S. T., Ng, N. L., Petaja, T., Pierce, J. R., Rasch, P. J., Roldin, P., Seinfeld, J. H., Shilling, J., Smith, J. N., Thornton, J. A., Volkamer, R., Wang, J., Worsnop, D. R., Zaveri, R. A., Zelenyuk, A., and Zhang, Q.: Recent advances in understanding secondary organic aerosol: Implications for global climate forcing, Rev. Geophys., 55, 509–559, https://doi.org/10.1002/2016rg000540, 2017.

Stone, D., Whalley, L. K., and Heard, D. E.: Tropospheric OH and $HO_2$ radicals: field measurements and model comparisons, Chem. Soc. Rev., 41, 6348–6404, https://doi.org/10.1039/c2cs35140d, 2012.

Vereecken, L., Novelli, A., and Taraborrelli, D.: Unimolecular decay strongly limits the atmospheric impact of Criegee intermediates, Phys. Chem. Chem. Phys., 19, 31599–31612, https://doi.org/10.1039/c7cp05541b, 2017.

Wang, Y., Zhao, Y., Li, Z., Li, C., Yan, N., and Xiao, H.: Importance of hydroxyl radical chemistry in isoprene suppression of particle formation from $\alpha$-pinene ozonolysis, ACS Earth Space Chem., 5, 487–499, https://doi.org/10.1021/acsearthspacechem.0c00294, 2021.

Wolfe, G. M.: AirChem/F0AM, GitHub [code], https://github.com/AirChem/F0AM.git (last access: 18 October 2024), 2024.

Wolfe, G. M., Marvin, M. R., Roberts, S. J., Travis, K. R., and Liao, J.: The Framework for 0-D Atmospheric Modeling (F0AM) v3.1, Geosci. Model Dev., 9, 3309–3319, https://doi.org/10.5194/gmd-9-3309-2016, 2016.

Xu, L., Møller, K. H., Crounse, J. D., Otkjær, R. V., Kjaergaard, H. G., and Wennberg, P. O.: Unimolecular reactions of peroxy radicals formed in the oxidation of $\alpha$-pinene and $\beta$-pinene by hydroxyl radicals, J. Phys. Chem. A, 123, 1661–1674, https://doi.org/10.1021/acs.jpca.8b11726, 2019.

Zang, H., Huang, D., Zhong, J., Li, Z., Li, C., Xiao, H., and Zhao, Y.: Direct probing of acylperoxy radicals during ozonolysis of $\alpha$-pinene: constraints on radical chemistry and production of highly oxygenated organic molecules, Atmos. Chem. Phys., 23, 12691–12705, https://doi.org/10.5194/acp-23-12691-2023, 2023.

Zhang, H., Yee, L. D., Lee, B. H., Curtis, M. P., Worton, D. R., Isaacman-VanWertz, G., Offenberg, J. H., Lewandowski, M., Kleindienst, T. E., Beaver, M. R., Holder, A. L., Lonneman, W. A., Docherty, K. S., Jaoui, M., Pye, H. O. T., Hu, W., Day, D. A., Campuzano-Jost, P., Jimenez, J. L., Guo, H., Weber, R. J., de Gouw, J., Koss, A. R., Edgerton, E. S., Brune, W., Mohr, C., Lopez-Hilfiker, F. D., Lutz, A., Kreisberg, N. M., Spielman, S. R., Hering, S. V., Wilson, K. R., Thornton, J. A., and Goldstein, A. H.: Monoterpenes are the largest source of summertime organic aerosol in the southeastern United States, P. Natl. Acad. Sci. USA, 115, 2038–2043, https://doi.org/10.1073/pnas.1717513115, 2018.

Zhang, X., McVay, R. C., Huang, D. D., Dalleska, N. F., Aumont, B., Flagan, R. C., and Seinfeld, J. H.: Formation and evolution of molecular products in $\alpha$-pinene secondary organic aerosol, P. Natl. Acad. Sci. USA, 112, 14168–14173, https://doi.org/10.1073/pnas.1517742112, 2015.

Zhang, Y., Peräkylä, O., Yan, C., Heikkinen, L., Äijälä, M., Daellenbach, K. R., Zha, Q., Riva, M., Garmash, O., Junninen, H., Paatero, P., Worsnop, D., and Ehn, M.: Insights into atmospheric oxidation processes by performing factor analyses on subranges of mass spectra, Atmos. Chem. Phys., 20, 5945–5961, https://doi.org/10.5194/acp-20-5945-2020, 2020.

Zhao, Y., Thornton, J. A., and Pye, H. O. T.: Quantitative constraints on autoxidation and dimer formation from direct probing of monoterpene-derived peroxy radical chemistry, P. Natl. Acad. Sci. USA, 115, 12142–12147, https://doi.org/10.1073/pnas.1812147115, 2018.

Zhao, Y., Yao, M., Wang, Y., Li, Z., Wang, S., Li, C., and Xiao, H.: Acylperoxy radicals as key intermediates in the formation of dimeric compounds in $\alpha$-pinene secondary organic aerosol, Environ. Sci. Technol., 56, 14249–14261, https://doi.org/10.1021/acs.est.2c02090, 2022.

Zhao, Z., Zhang, W., Alexander, T., Zhang, X., Martin, D. B. C., and Zhang, H.: Isolating alpha-pinene ozonolysis pathways reveals new insights into peroxy radical chemistry and secondary organic aerosol formation, Environ. Sci. Technol., 55, 6700–6709, https://doi.org/10.1021/acs.est.1c02107, 2021.